SECOND EUROPEAN CONFERENCE ON EARTHQUAKE ENGINEERING
AND SEISMOLOGY, ISTANBUL AUG. 25-29, 2014

A PREDICTIVE MODEL FOR MAXIMUM INTERSTORY DRIFT RATIO FOR CODE COMPLYING LOW AND MID RISE FRAME-TYPE REGULAR RC BUILDINGS IN TURKEY

Tuba EROĞLU AZAK[1] and Sinan AKKAR[2]

ABSTRACT

Seismic performance of buildings is of prime importance when future earthquakes are of concern. This fact urges the implementation of rational seismic design and assessment methodologies to ensure the safe and reliable response of existing and new buildings against seismic action. Quantification of seismic reliability of structures has always been a challenging task for structural engineers due to randomness and uncertainties involved in the earthquake phenomenon and nonlinear structural response. This fact motivated many researchers to propose methodologies under the framework of performance-based earthquake engineering. One of the major outcomes in this area is Probabilistic Seismic Demand Analysis concept that aims at estimating the annual frequency exceeding a defined level of a structural demand parameter. One of the approaches to carry out Probabilistic Seismic Demand Analysis requires structure-specific predictive models for the selected engineering demand parameter. This paper proposes a predictive model for maximum interstory drift ratio (MIDR) for code-confirming low- and mid-rise reinforced concrete frame type Turkish buildings. The proposed MIDR predictive model that is developed as a function of moment magnitude, source-to-site distance, stiff and soft site conditions, and strength reduction factor produces median MIDR estimations and considers the aleatory variability (record-to-record variability) with a standard deviation. In this sense, it is believed that the proposed MIDR predictive model can meet the current engineering needs in terms of probabilistic seismic performance assessment of existing as well as new buildings.

INTRODUCTION

The main objective of performance-based earthquake engineering (PBEE) is to ensure the expected structural behavior by satisfying target performance levels with realistic quantification of seismic demand and structural capacity through the incorporation of randomness in seismic action and uncertainties in structural response. This probabilistic framework enables the estimation of performance objectives in terms of exceedance probabilities of engineering demand parameters (EDPs).

Estimating EDPs in a fully probabilistic manner for a given annual exceedance rate is initially presented by Bazzuro (1998) under the probabilistic seismic demand analysis (PSDA) concept. PSDA can be carried out by following different approaches (Shome and Cornell, 1999). One of the methods is based on the estimation of structural demands (EDPs) through predictive models that make use of seismological estimator parameters (Shome and Cornell, 1999). This paper further improves the aforementioned PSDA concept by including a structural parameter in the structure-specific predictive

[1] Research Assistant, Department of Civil Engineering, Akdeniz University, Antalya, tuba.eroglu@gmail.com
[2] Professor, Boğaziçi University, Kandilli Observatory and Earthquake Research Institute, İstanbul, sinan.akkar@boun.edu.tr

model for increasing the accuracy of EDP estimations. The structural parameter selected for this purpose is strength reduction factor as an efficient structural estimator parameter to be used in a simplified predictive model should be robust and easy-to-compute for accurate representation of the nonlinear structural response. The EDP chosen in this study is maximum interstory drift ratio (MIDR) as it correlates well with structural damage and it is used extensively in current seismic design and rehabilitation guidelines.

The frames utilized in this paper are extracted from 3-D RC buildings that are capable of reflecting the common Turkish construction practice. In order to estimate MIDR demands, nonlinear response history analyses (RHA) are performed under the chosen ground-motion database. Under the light of the collected results and investigations on influence of several structural and seismological parameters on MIDR demands, the MIDR predictive model is developed as a function of moment magnitude (M_w), source-to-site distance (R_{jb}), stiff and soft site conditions (NEHRP C and D) and strength reduction factor (R_y). The likely uncertainties of these independent estimator parameters as well as their interaction are addressed by the standard deviation of the MIDR predictive model. On the basis of the log-normality assumption of MIDR demands, the derived predictive model describes the probability distribution of MIDR conditioned on the chosen ground-motion and structural parameters. The major advantage of this approach is the direct estimation of MIDR from independent structural and seismological variables. Accordingly, the MIDR model presented in this study is believed to serve as a useful tool for seismic performance assessment applications in accordance with PBEE objectives.

STRONG MOTION DATABASE

The accelerograms utilized in this study are obtained from three sources: PEER strong-motion database (http://peer.berkeley.edu/smcat/), European strong-motion database (http://www.isesd.hi.is/ESD_Local/frameset.htm) and Turkish strong-motion database (http://kyh.deprem.gov.tr/ftpe.htm). A total of 628 unscaled records (314 two-component horizontal accelerograms) are utilized for nonlinear response history analyses. The ground motion database consists of earthquakes with normal, strike-slip and reverse faulting mechanism. The NEHRP C and D site classes can be classified by $V_{s,30}$ values (average shear wave velocity of the upper 30 soil profile) with 360 m/s $\leq V_{s,30} <$ 760 m/s and 180 m/s $\leq V_{s,30} <$ 360 m/s, respectively. The moment magnitude (M_w) range of the database is $5.0 \leq M_w < 7.7$ whereas all records have Joyner-Boore distances (R_{jb}; Joyner and Boore, 1981) that are less than 100 km. The chosen magnitude and distance range is believed to have engineering significance for seismic design and performance assessment of new and existing buildings.

ANALYTICAL MODELS

In order to resemble the Turkish building stock, 3-D buildings are generated first on the basis of a statistical study that compiles general characteristics of the Turkish RC residential buildings. The 3-D buildings are designed using the PROBINA Orion software (Prota, 2008) version 14.1 in accordance with the Turkish standards; TS 500-2000 (Turkish Standards Institute, 2000), TS 498 (Turkish Standards Institute, 1997) and Turkish Earthquake Code (TEC, 2007). The buildings are assumed to be located at a site in Zone I with Z3 (soft soil) site classification. All models are designed for ductile behavior using R=8 as suggested by Turkish Earthquake Code (TEC, 2007). The effective peak acceleration for design spectrum is taken as A_0=0.4g and the resulting spectral ordinates correspond to a return period of T_R=475 years according to the provisions in this code. From each 3-D building an interior frame is selected among continuous frames as a representative one for further analysis. The frame models of interest have story numbers ranging between 3 and 9 stories with fundamental periods (T_1) ranging from 0.7s to 1.4s. The details of the analytical models as well as statistical study of the Turkish RC residential buildings can be found in Eroglu Azak (2013).

The selected frames are analytically modeled using OpenSees (2006) finite element analysis software with fiber-based beam-column elements. For each section in the analytical frame models, the unconfined concrete and confined concrete model properties are calculated according to the modified

Kent and Park model (1971) using unconfined compressive strength with σ_c=20 MPa at ε_{c0}=0.002. The elastic perfectly plastic (EPP) steel material is defined with a yield strength of 420 MPa at ε_{sy}=0.0021 yield strain.

In order to estimate the MIDR demands, nonlinear response history analyses (RHA) are performed using the RC frame set. A total of 3768 nonlinear RHA are carried out. The collected results from nonlinear RHA indicate the significance of seismicity level, randomness of earthquakes and uncertainties in structural response. This observation indicates that one should account for these factors in order to evaluate nonlinear structural response in a reliable manner. The nonlinear RHA results will be discussed in the subsequent sections.

In addition to nonlinear RHA, nonlinear static analyses are also carried out by applying a first mode compatible lateral load pattern. The idealizations of pushover curves is done using ATC-40 (ATC, 1996) procedure. Idealized equivalent SDOF systems are used for running linear RHA. The elastic pseudo spectral accelerations (PSA_e) computed from these analyses are used together with the previously defined yield pseudo spectral accelerations (PSA_y) from bilinear idealizations to compute strength reduction factor, (R_y) for each case. Eq. (1) shows the definition of R_y used in this study.

$$R_y = \frac{PSA_e}{PSA_y} \tag{1}$$

INTERPRETATION OF ANALYSIS RESULTS

After computing MIDR demands using nonlinear RHA results, for each earthquake record maximum of two horizontal components are taken for further analysis as it possesses the most critical value for engineering design and assessment. The collected MIDR demands are first investigated for log-normality assumption. After that, the influence of some prominent seismological and structural parameters on nonlinear MIDR demands are investigated.

Log-normality of MIDR

The distribution of MIDR is important for the proposed predictive equation in this study. In general, ground-motion parameters are assumed to be log-normally distributed (Baker and Cornell, 2006; Bommer and Abrahamson, 2006; Jayaram and Baker, 2008). Similarly MIDR demands are assumed to be log-normally distributed in several studies (Song and Ellingwood, 1999; Shome and Cornell, 1999). Recently Romão et al. (2011) expressed the suitability of log-normal distribution for MIDR for a given level of the intensity measure (IM). More specifically, Romão et al. (2011) indicated that the MIDR demands calculated from a set of ground motions scaled according to a selected IM follow log-normal distribution. Bearing on this assertion, the distribution of MIDR is verified for log-normality using Kolmogorov-Smirnov goodness-of-fit test (Ang and Tang, 1975) at a significance level of α_{sig}=5%.

In order to figure out the limits that define the deviation of MIDR demands from log-normal distribution, the logarithm of MIDR inventory is inspected by normal quantile (Q-Q) plots. Figure 1 illustrates the normal Q-Q plots for 3- and 4- story frame models. The plots are given in this figure indicate that, except for the tails, MIDR can be assumed as log-normally distributed, the standard normal distributions of the logarithms of MIDR values are very close to the theoretical standard normal distribution within ± 2 standard deviation (σ) range. Under these observations, the log-normality of MIDR assumption is assumed to be sufficient for the MIDR predictive model and its implementation to the probability-based procedures. The log-normality assumption holds for the rest of the frame set however the related scatters are not given here for brevity.

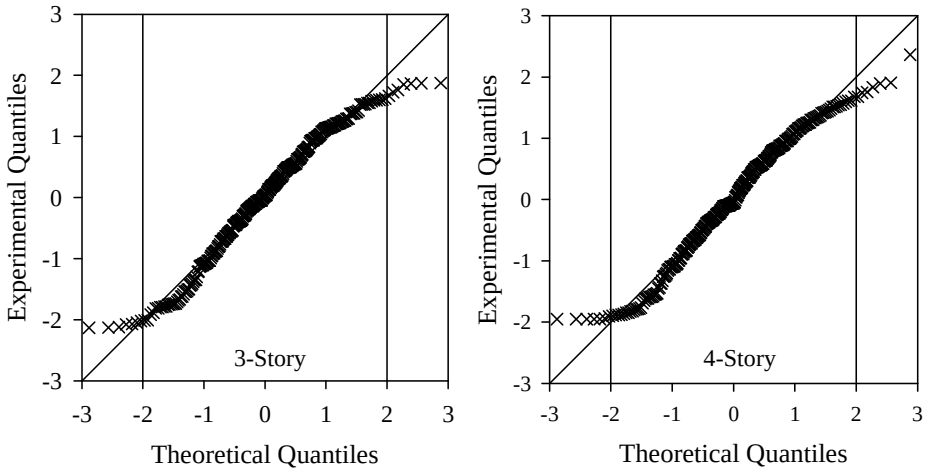

Figure 1. Normal Q-Q plots for the logarithmic MIDR demands for the 3- and 4- story frames

Effect of Various Structural and Seismological Parameters on MIDR Demands

Dependence of MIDR on Fundamental Period and Number of Stories

The MIDR demands of model frames are presented in terms of their fundamental period (T_1) and total height in Figures 2a and 2b, respectively. The solid squares on these figures correspond to median (logarithmic mean) MIDR values for each frame model. The logarithmic standard deviation of MIDR results for each building is indicated under the corresponding scatter column. Figure 2 shows that median MIDR values tend to decrease with increasing fundamental period and story height. However, the variation of MIDR with the changes in building period and height seems to be negligible for the building models considered in this study. Thus, one may assume that MIDR is independent of building fundamental period and height as long as the dynamic response of considered buildings is of concern in this study. The similarity in dispersion statistics fortifies this remark.

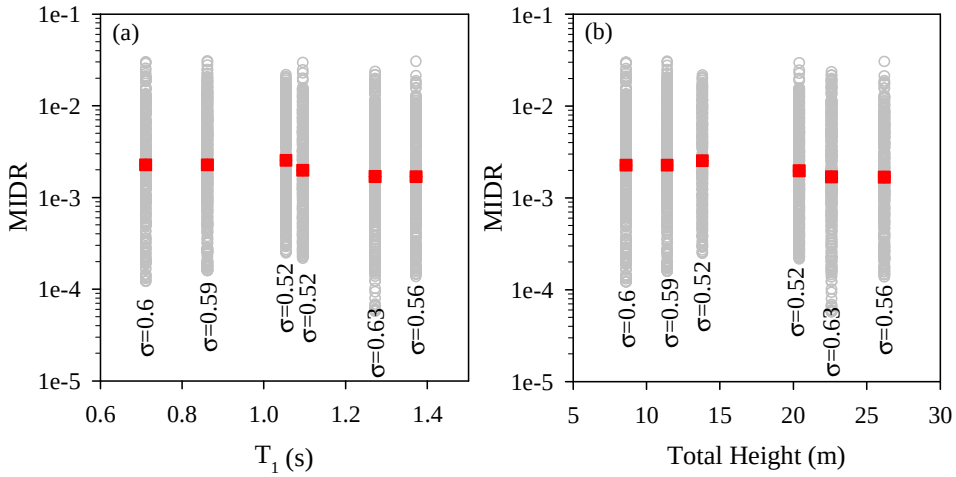

Figure 2. Dependency of MIDR on (a) fundamental period and (b) total height. The solid squares represent the median values of each frame model. The MIDR logarithmic standard deviations (σ) of each model are also given on these plots.

In order to provide a quantitative measure about the dependence of MIDR on T_1 and story number ANOVA tests are implemented using the nonlinear RHA results in hand. The ANOVA results that are computed for different magnitude and distance bins are given in Table 1. The p-value statistics listed in this table are mostly above 0.05 and would suggest the insensitivity of MIDR on building fundamental period for the building type and period range covered in this study. This observation is used while developing the proposed predictive model. In other words, only one specific expression for estimating MIDR is developed instead of multiple equations that account for the variations in story number or fundamental period.

Table 1. Results of ANOVA tests in terms of magnitude and distance sub-bins (grey shaded cells show the results where null-hypothesis, independency of MIDR on T_1 and building height, cannot be rejected)

M_w	5.0-5.5	5.5-6.0	6.0-6.5	6.5-7.0	7.0-7.7					
p value ANOVA	0.33	0.22	0.31	0.16	0.14					
R_{jb} (km)	0-10	10-20	20-30	30-40	40-50	50-60	60-70	70-80	80-90	90-100
p value ANOVA	0.01	0.30	0.31	0.14	0.91	0.29	0.63	0.94	0.93	0.94

Style-of-Faulting (SoF) Effect

Confined to the building models and ground-motion database of this study, observations about the independency of MIDR on fundamental period imply the use of entire nonlinear RHA results to produce more compact statistics on the influence of considered seismological and structural parameters on MIDR demands. Figure 3 shows the variation of entire MIDR values as a function of distance and magnitude for normal, reverse and strike-slip faulting mechanisms. The scatter plots suggest the existence of SoF influence on MIDR. However, the nonuniform distribution of SoF in terms of magnitude and distance in the ground-motion dataset as well as the interaction between ground motion and building response requires a statistical quantification about the significance of SoF on MIDR. This is achieved through ANOVA tests similar to the previous section. The magnitude bins used in ANOVA tests are established as; M_w 5.0-5.5, M_w 5.5-6.0, M_w 6.0-6.5, M_w 6.5-7.0 and M_w 7.0-7.7. The distance bins have increments of 20 km. A total of 5 distance bins are established with the following ranges: 0-20 km, 20-40 km, 40-60 km, 60-80 km and 80-100 km. For each magnitude-distance bin, the sample means of grouped data according to the SoF are compared. Although not shown here for brevity, the ANOVA tests indicate that SoF effect is visible only for a few number of magnitude distance bin pairs compared to the entire number of tests at 5% significance level.

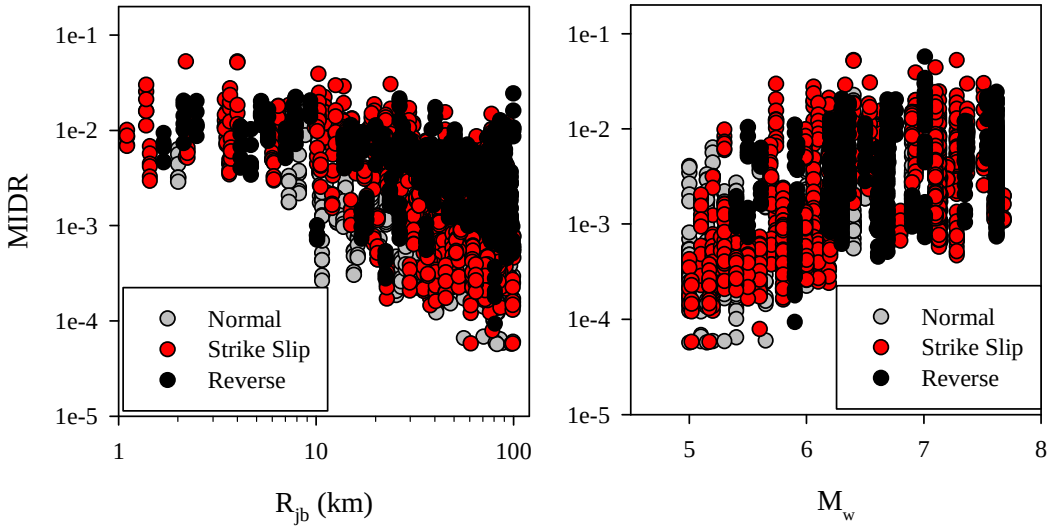

Figure 3. Influence of SoF on MIDR

Based on the ANOVA test results, one can suggest a weak dependence of MIDR on SoF. The lack of data in several magnitude-distance bins as well as the nonuniform distribution of the data in terms of SoF may cost doubts about the reliability of the conclusion derived from ANOVA tests. For the sake of simplicity, the predictive model presented in this study disregards the influence of SoF on MIDR estimations and this simplification may result in a slight bias in the estimated MIDR values. This bias is accepted as tolerable and disregarding SoF effects on MIDR is considered as the limitation of the proposed empirical model.

Effect of Soft and Stiff Site Conditions

The site condition effect on MIDR demands are confined to the NEHRP C and D site classes only. The absence of other site conditions, such as rock sites with $V_{s,30} \geq 760$m/s, in the database may result in limited observations about the actual soil influence on MIDR. However, the site classes encompassed by the database represent the most frequent soil conditions for many engineered buildings. The scatters in Figure 4 show the variation of MIDR for the site classes considered in this study. Figure 4a shows this variation as a function of distance whereas Figure 4b gives the same information in terms of magnitude. The MIDR data pertaining to NEHRP C and D sites are shown in different color codes on these panels. The plots indicate that MIDR values are not very sensitive to the soil behavior of NEHRP C and D site classes as their magnitude- and distance-dependent trends are similar to each other without showing a significant quantitative variation. In other words, there is no clear separation of MIDR demands between NEHRP C and D site classes. ANOVA tests are done to see the sensitivity of MIDR on site classes. The same magnitude-distance bin pairs are used for the current ANOVA tests. The only difference is the grouping of MIDR values: for the current analysis logarithmic means of MIDR values are given for NEHRP C and NEHRP D site classes. The ANOVA test results, not shown here for brevity, do not exhibit a strong evidence for speculating on the dominance of soil behavior (NEHRP C and D site classes) on MIDR amplitudes. However, when compared to ANOVA statistics for SoF, the site class seems to play a more dominant role in the MIDR amplitudes as there are more magnitude-distance bin pairs that show the significance of site class effect on sample mean MIDR values. Moreover, the distribution of data in terms of site class for the selected magnitude and distance bin pairs seem to be more uniform.

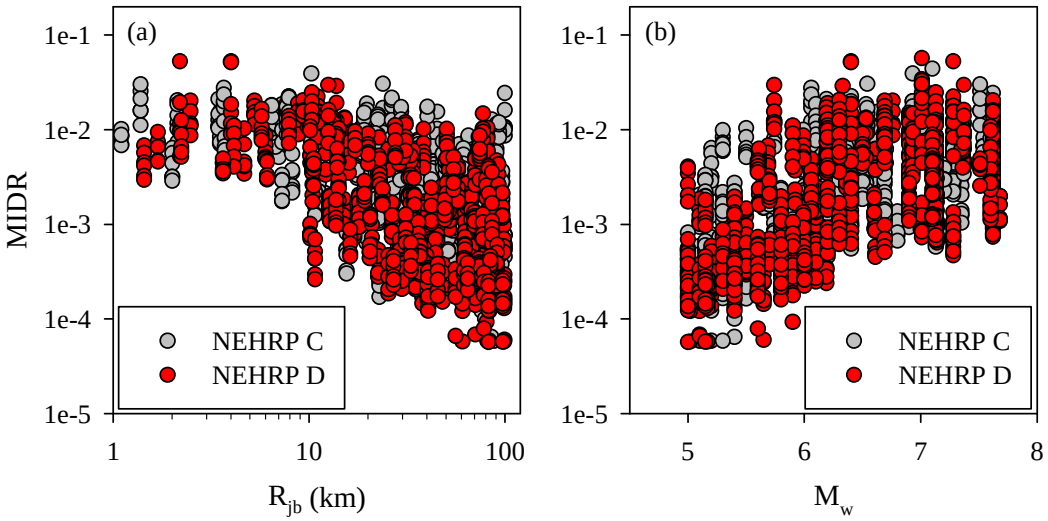

Figure 4. Variation of MIDR as functions of (a) distance and (b) magnitude bins for different site classes

Variation of MIDR with Distance and Magnitude

Figures 5 and 6 present two-way statistical plots for different magnitude and distance bin pairs using the entire MIDR inventory. Each scatter plot contains trend lines that show the general behavior of MIDR for the two adjacent magnitude or distance bins. The increase in magnitude decreases the distance-dependent decay rate in MIDR that can be observed in Figure 5. This figure also shows the insensitivity of MIDR for large magnitude and short distance records. The scatters in Figure 6 that show the magnitude-dependent MIDR variation for different distance bins emphasize this observation from another perspective. These plots suggest that MIDR changes gradually for $M_w > 6.0$ for distances up to 40 km. For smaller magnitude events and for larger distances (distances greater than 50 km), the observed changes in MIDR demands are very rapid. In general the magnitude scaling of MIDR can be represented by a 2nd order polynomial. The distance scaling of MIDR requires a magnitude-dependent slope. These conclusions will be used while establishing the functional form of the proposed MIDR predictive model.

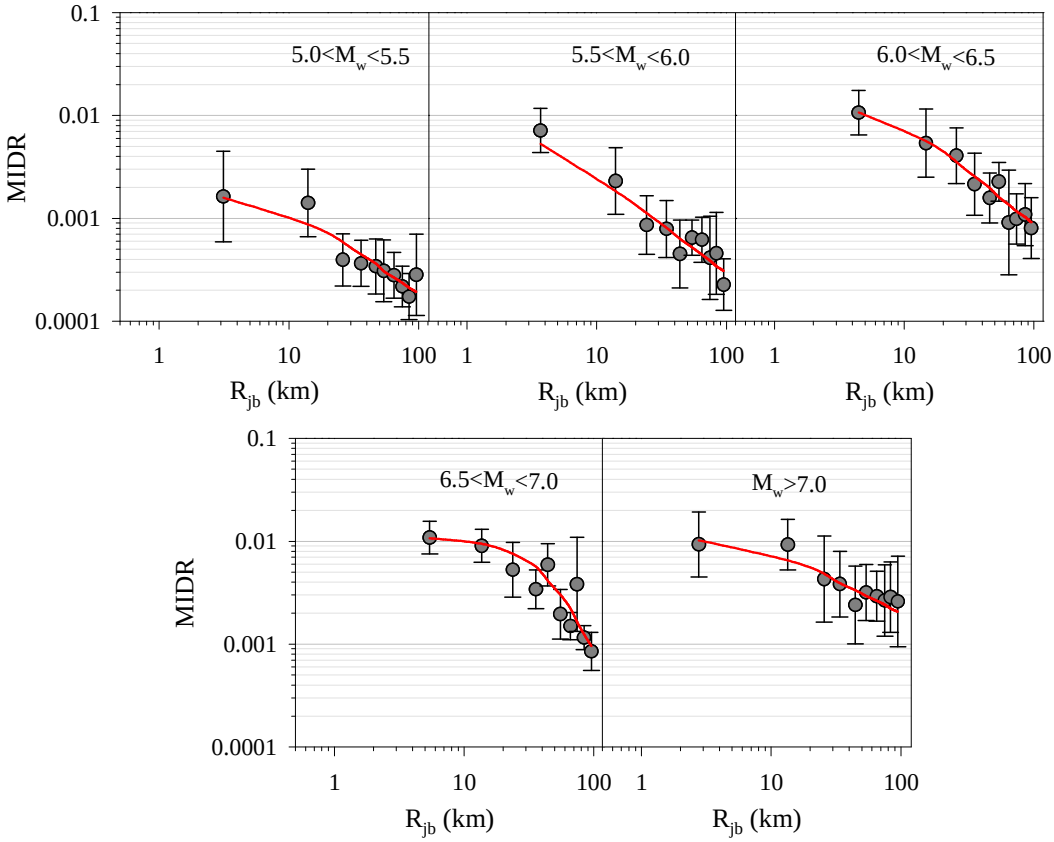

Figure 5. Variation of median MIDR together with ± 1 standard deviation error bars against distance for different magnitude bins. The solid lines are nonlinear fits to show the overall trend in MIDR variation

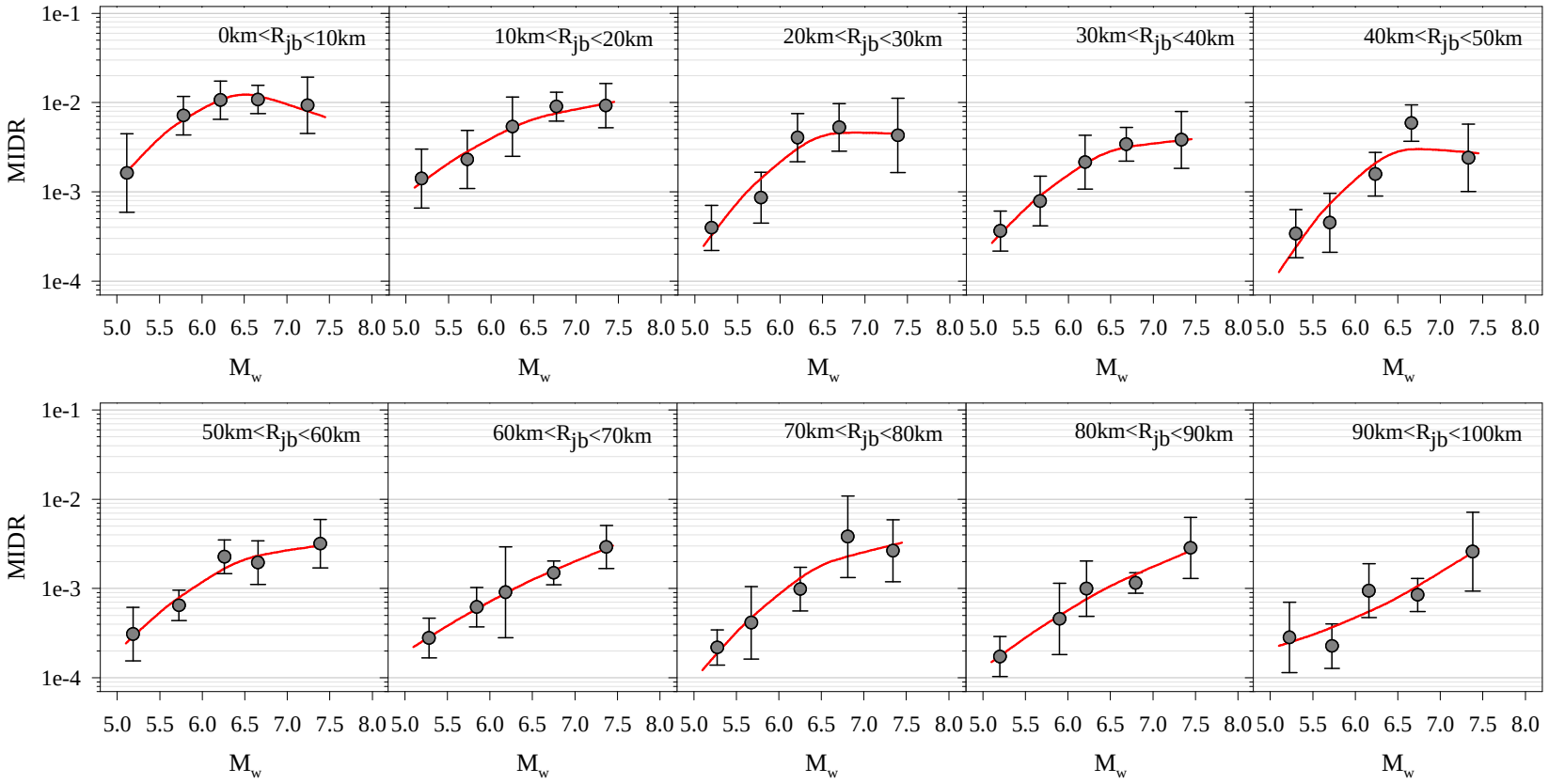

Figure 6. Variation of median MIDR together with ± 1 standard deviation error bars against magnitude for different distance bins. The solid lines are nonlinear fits to show the overall trend in MIDR variation

Relationship between MIDR and Strength Reduction Factor

Figure 7 illustrates the relationship between strength reduction factor and MIDR. There is a fairly good correlation between R_y and MIDR for $R_y \geq 0.05$. This agreement diminishes towards very small R_y values (i.e., $R_y < 0.05$). It is believed that the dominancy of gravitational loads over seismic loads is the reason behind the almost steady MIDR values against decreasing strength reduction factors for $R_y<0.05$. In other words, the small-magnitude and far-source recordings that result in negligible seismic demands do not govern the lateral deformation shape of buildings. Instead, gravitational loads dominate the structural behavior for such recordings. This fact results in the observed pattern for R_y that is presented in Figure 7.

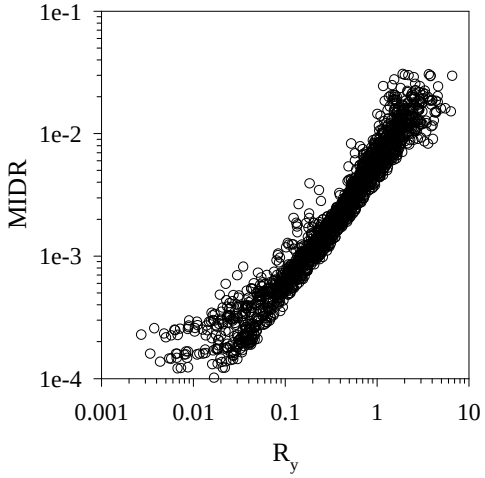

Figure 7. Dependence of MIDR on R_y using entire database

FUNCTIONAL FORM OF THE PREDICTIVE MODEL

Based on the observations summarized in the previous sections and the correlation of MIDR with structural and ground-motion parameters, the predictive model is developed as a function of magnitude (M_w), source-to-site distance (R_{jb}), site conditions, strength reduction factor (R_y). The proposed predictive model for MIDR is selected among several functional forms considering the success and stability of the model in predicting nonlinear MIDR demands. The functional form of MIDR is given in Eq. (2). The predictive model produces median MIDR (logarithmic mean) estimations and considers the aleatory variability (record-to-record variability) with the standard deviation (sigma) term, $\sigma_{\log10(MIDR)}$.

$$\log_{10}(\text{MIDR}) = b_1 + b_2 M_w + (b_3 + b_4 M_w)\log_{10}(D) + b_6 \log_{10}(F) + b_8 S_1 + b_9 S_2 + \sigma_{\log10(MIDR)} \quad (2)$$

$$D = \sqrt{R_{jb}^{\,2} + b_5^{\,2}}$$

$$F = \sqrt{R_y^{\,2} + b_7^{\,2}}$$

where,

b_1 to b_9 are regression constants
M_w is moment magnitude
R_{jb} is Joyner and Boore distance
R_y is strength reduction factor
S_1=1 for soft soil (NEHRP D) and 0 otherwise
S_2=1 for stiff soil (NEHRP C) and 0 otherwise

The dispersion about median MIDR is presented by standard deviation, $\sigma_{\log10(MIDR)}$, that considers the inter-event (σ_2) and intra-event (σ_1) variability. The inter-event variability defines the variations due to specific source features of earthquakes. The intra-event variability accounts for the variations of path and site effects within an earthquake. The intra-event standard deviation given for the proposed MIDR model also considers the variation of total story number (or fundamental period)

since each building model is assumed as a separate site collocated closely to the recording station while running the regressions. The total standard deviation expression is given in Eq. (3) and it is calculated as 0.1195.

$$\sigma_{\log10(MIDR)} = \sqrt{\sigma_1^{\,2} + \sigma_2^{\,2}} \tag{3}$$

The functional form given by Eq. (3) contains a linear magnitude scaling term ($b_1+b_2M_w$). The distance scaling term is also linear with a magnitude-dependent slope [$(b_3+b_4M_w)\log_{10}D$] to account for the influence of magnitude on the MIDR variation with increasing or decreasing distance. The expressions used to define magnitude and distance scaling are developed by considering the magnitude and distance-dependent variation of MIDR. The influence of structural parameter, R_y, is described in by $b_6\log_{10}(F)$ term that is also identified from the relationships between MIDR versus R_y. The influence of site class (either NEHRP C or NEHRP D due to the limitation of the strong-motion database) is defined by the dummy site variables S_1 and S_2 in Eq. (2) that take values of unity when the MIDR is estimated for NEHRP D (S_1=1) and NEHRP C (S_2=1) site classes. Thus, the proposed MIDR predictive model does not account for the nonlinear soil effects on the median MIDR estimations.

The regressions are done by using the one-stage maximum likelihood method of Joyner and Boore (1993). The regression method computes the coefficients by considering the functional forms of each estimator parameter obtained from observations. The uncertainties involved in the functional forms of each estimator parameter is accounted for by this regression technique and it is reflected on the computed standard deviation. The regression constants of the predictive model are given in Table 2.

Table 2. Equation constants of the MIDR predictive model

b_1	b_2	b_3	b_4	b_5	b_6	b_7	b_8	b_9	σ_1	σ_2
-1.0461	0.00543	-0.29536	0.02325	7.22157	0.92186	0.02929	-1.01252	-1.04103	0.1167	0.0259

EVALUATION OF THE PREDICTIVE MODEL

The performance of the proposed model is investigated by considering the conventional residual analysis plots. These are given in Figure 8 and they show the variation of total residuals in terms of magnitude (M_w), source-to-site distance (R_{jb}) and strength reduction factor (R_y). The plots depict that MIDR estimations are unbiased in terms of M_w, R_{jb} and R_y, which complies with the efficiency condition described by Luco and Cornell (2007).

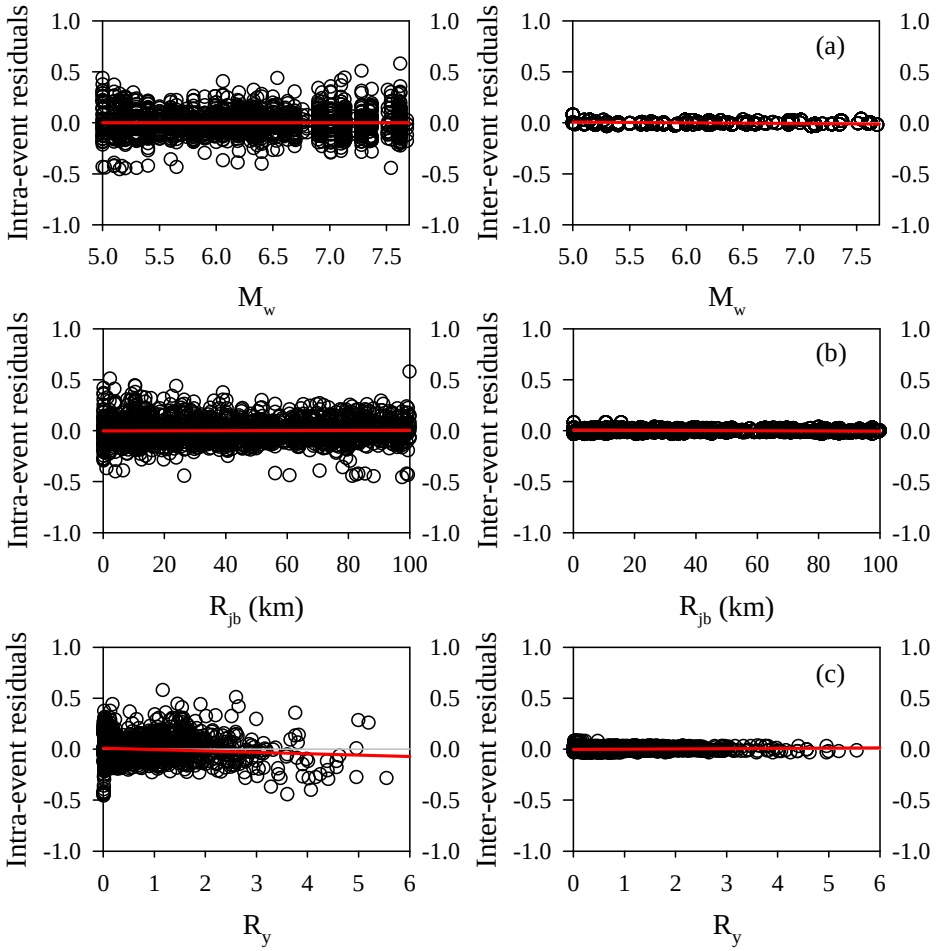

Figure 8. Residual plots of the predictive model in terms of (a) M_w, (b) R_{jb} and (c) R_y. The overall trends of the residuals are shown with red lines; a 2nd order fit on the residual scatters

Figure 9 shows the variation of median MIDR demands in terms of source-to-site distance. The figure presents the median MIDR demands for different strength reduction factors (R_y). The soil condition chosen for these plots is NEHRP site class C (360m/s ≤ $V_{s,30}$ < 760m/s). The plots clearly indicate the level of sensitivity of MIDR on magnitude, distance and nonlinear structural behavior. As one can infer from the figure, the increase in magnitude and level of nonlinearity amplifies the MIDR demands and median MIDR estimations decrease with increasing distance.

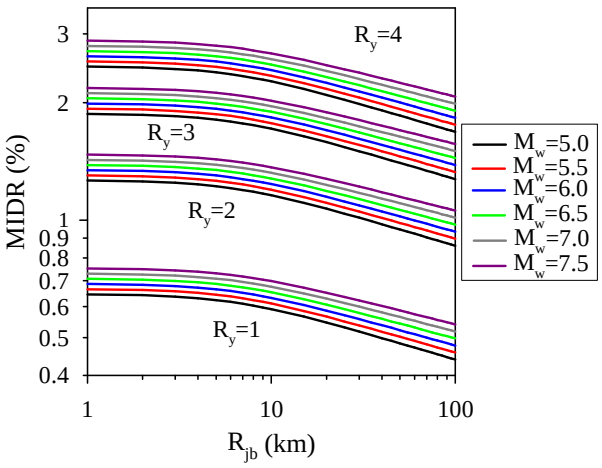

Figure 9. Variation of median MIDR estimations with R_{jb} for R_y=1, 2, 3 and 4

LIMITATIONS AND GENERAL FEATURES OF THE PROPOSED MIDR MODEL

The overall features of the MIDR predictive model as well as its capabilities and assumptions made during its development are listed below.

- The predictive model is developed for code complying low- and mid-rise (3 to 9 story) RC buildings. The period range of the frames vary between ~0.7s and 1.4s. Further studies are necessary to assess the performance of the proposed model for high-rise and stiffer buildings. Due to the limitations of 2-D modeling, torsional effects are not included in the study. Moreover the model is developed assuming that the buildings are dominated by first-mode behavior.

- The magnitude range of the MIDR model is $5.0 \leq M_w < 7.7$. The source-to-site distance (R_{jb}) is confined to $R_{jb} \leq 100$ km. To this end, the proposed predictive model addresses both near and far distance as well as small and large magnitude events of engineering interest.

- The ground-motion set is a composition of accelerograms that are recorded on stiff (NEHRP C) and soft (NEHRP D) site classes. The range of applicability of the MIDR model is between 180 m/s and 760 m/s in terms of $V_{s,30}$. Although this shear-wave velocity range covers the soil conditions of most engineered structures, the MIDR demands for buildings located on rock sites should be integrated in future studies related to this model.

- The proposed model is capable of estimating nonlinear MIDR demands for code-complying moment resisting frames.

CONCLUSIONS

The major advantage of the MIDR predictive equation presented in this study is the direct estimation of EDP from independent structural and seismological variables. This feature is particularly useful for the probabilistic seismic performance and damage assessment of structural systems by using MIDR as the major EDP. In essence, the PSDA approach favored in this study does not utilize ground-motion IMs (e.g., pseudo spectral acceleration, pseudo spectral velocity) as intermediate variables between seismic hazard and structural response and it provides a practical methodology by direct estimation of EDPs from seismological and structural parameters. As indicated, the likely uncertainties of these independent estimator parameters as well as their interaction are addressed by the standard deviation of the EDP predictive model. To this end, the proposed MIDR predictive model is believed to be useful in realistic quantification of seismic demands in terms of MIDR. The major contribution of this study besides the MIDR model is the improvement in the PSDA methodology through implementation a structural parameter into the predictive model of the selected EDP.

REFERENCES

Ang AH-S, and Tang WH, (1975) Probability concepts in engineering planning and design, Vol 1, New York, Wiley.

Applied Technology Council, ATC (1996) ATC-40, Seismic evaluation and retrofit of concrete buildings, Report No: SSC 96-01, Redwood City, CA.

Baker JW, and Cornell CA, (2006) "Spectral shape, record selection and epsilon", *Earthquake Engineering and Structural Dynamics*, Vol. 35(9), 1077-1095.

Bazzurro P, (1998) Probabilistic seismic demand analysis, Ph.D. Thesis, Stanford University, Stanford, CA, 329 pages.

Bommer JJ, and Abrahamson NA, (2006) "Why do modem probabilistic seismic-hazard analyses often lead to increased hazard estimates?", *Bulletin of the Seismological Society of America*, Vol. 96(6), 1967-1977.

Cornell CA, (1968) "Engineering seismic risk analysis", *Bulletin of the Seismological Society of America*, Vol. 58(5), 1583-1606.

Eroğlu Azak T, (2013) A Predictive Model for Maximum Interstory Drift Ratio (MIDR) and its Implementation in Probability-based Design and Performance Assessment Procedures, Ph.D. Thesis, Middle East Technical University, Ankara, Turkey, 242 pages.

Jayaram N, and Baker JW, (2008) "Statistical tests of the joint distribution of spectral acceleration values", *Bulletin of the Seismological Society of America*, Vol. 98(5), 2231-2243.

Joyner WB, and Boore DM, (1981) "Peak horizontal acceleration and velocity from strong-motion records including records from the 1979 Imperial Valley, California, Earthquake", *Bulletin of the Seismological Society of America*, Vol. 71(6), 2011-2038.

Joyner WB, and Boore DM, (1993) "Methods for regression analysis of strong-motion data", *Bulletin of the Seismological Society of America*, Vol. 83(2), 469-487.

Kent DC, and Park R, (1971) "Flexural Members with Confined Concrete", *Journal of Structural Division, ASCE*, Vol. 97(7), 1969-1990.

Luco N, and Cornell, CA, (2007) "Structure-specific scalar intensity measures for near-source and ordinary earthquake ground motions", *Earthquake Spectra*, Vol. 23(2), 357-392.

OpenSees Development Team, (2006) OpenSees: Open System for Earthquake Engineering Simulation Manual, OpenSees version: 2.0.0, Pacific Earthquake Engineering Research Center, University of California, Berkeley, California.

Prota, (2008) Probina Orion - Bina Tasarım Sistemi 2008, Teknik Özellikler, Ankara, Turkey.

Romão X, Delgado R, and Costa A, (2011) "Assessment of the statistical distributions of structural demand under earthquake loading", *Journal of Earthquake Engineering*, Vol. 15(5), 724-753.

Shome N, and Cornell CA, (1999) Probabilistic seismic demand analysis of nonlinear structures. Rep. No. RMS-35, Department of Civil and Environmental Engineering, Stanford University, Stanford, CA, 320 pages.

Song J, and Ellingwood BR, (1999) "Seismic reliability of special moment steel frames with welded connections II", *Journal of Structural Engineering*, Vol. 125(4), 372-384.

Turkish Standards Institute, (1997) TS 498, Design loads for buildings, Ankara, Turkey.

Turkish Standards Institute, (2000) TS 500-2000 Requirements for Design and Construction of Reinforced Concrete Structures, Ankara, Turkey.

Turkish Earthquake Code, TEC (2007) Specification for Buildings to be Built in Seismic Zones, Ankara, Turkey, Ministry of Public Works and Settlement, Government of Republic of Turkey.